JBUON 2021; 26(2): 418-428
ISSN: 1107-0625, online ISSN: 2241-6293 • www.jbuon.com
Email: editorial_office@jbuon.com

ORIGINAL ARTICLE

miR-497 targets VEGF signal pathway to regulate proliferation, invasion and migration of hepatocellular carcinoma cells: a primary study using DEC-MRI

Tianyu Zhang[1]*, Guoxu Ding[2]*, Hao Wang[3], Haifeng Hu[4], Yuguang Wang[1], Hui Li[3], Hongwei Zhang[5], Li Wang[6], Wennan Lin[7], Liguo Hao[8], Bo Li[1], Chunlei Zheng[9], Youli Du[10], Lili Song[11]

[1]CT Department, The Second Affiliated Hospital of Qiqihar Medical College, Qiqihar 161000, China. [2]Party Committee Office Department, The Second Affiliated Hospital of Qiqihar Medical College, Qiqihar 161000, China. [3]Neuroelectrophysiology Department, The Second Affiliated Hospital of Qiqihar Medical College, Qiqihar 161000, China. [4]MRI Department, The Second Affiliated Hospital of Qiqihar Medical College, Qiqihar 161000, China. [5]Scientific Research Department, The Second Affiliated Hospital of Qiqihar Medical College, Qiqihar 161000, China. [6]Imaging Department, The Third Affiliated Hospital of Qiqihar Medical College, Qiqihar 161000, China. [7]All Departments, The Second Affiliated Hospital of Qiqihar Medical College, Qiqihar 161000, China. [8]Qiqihar Medical Imaging Technology College, Qiqihar 161000, China. [9]Oncology department, The Second Affiliated Hospital of Qiqihar Medical College, Qiqihar 161000, China. [10]In department, The Second Affiliated Hospital of Qiqihar Medical College, Qiqihar 161000, China. [11]Anesthesiology Department, The Third Affiliated Hospital of Qiqihar Medical College, Qiqihar 161000, China.

*Tianyu Zhang and Guoxu Ding contributed equally in this paper.

Summary

Purpose: *To quantify the expression of miR-497 and its target gene VEGF-B in patients with hepatocellular carcinoma (HCC), and microvascular invasion (MVI) to identify their relationship with clinicopathological characteristics and prognosis.*

Methods: *Imaging data of postoperative cancer and adjacent tissues of HCC patients with MVI diagnosed by dynamic contrast-enhanced magnetic resonance imaging (DCE-MRI) were retrospectively analyzed. The expression of miR-497 in clinical samples and HepG2 and SMMC-7721 cell lines was quantified by quantitative PCR (Q-PCR). Correlations between miR-497 and patient survival and VEGF-B were explored in TCGA database. The invasion and migration of SMMC-7721 cells were tested by transwell assay. The binding sites between miR-497 and its target gene VEGF-B were verified by dual-luciferase reporter (DLR) assay, and VEGF-B levels were analyzed by western blot (WB).*

Results: *miR-497 showed a lower expression in HCC patients with MVI than those without MVI. It was also lowly expressed in HCC cell lines compared to normal liver cell lines. The proliferation and migration in HCC cells were inhibited by overexpression of miR-497, which were enhanced after transfection with miR-497 inhibitor. miR-497 had an effect on VEGF-B levels and there was a regulatory relationship between them. miR-497 was able to target VEGF-B and downregulate the receptor of VEGF-B (FLT-1).*

Conclusion: *miR-497 was lowly expressed in HCC tissues, and its overexpression inhibited invasion and metastasis in HCC cells by suppressing VEGF-B levels. MiR-497 and its target gene VEGF-B are closely associated with the biological function and may serve as prognostic factors of MVI in patients with HCC.*

Key words: *miR-497, microvascular invasion, hepatocellular carcinoma, VEGF-B, invasion, migration*

Introduction

Hepatocellular carcinoma (HCC) is the most common primary tumor in the liver and the third fatal tumor worldwide. The tumor grows infiltratively and invades blood vessels to form metastatic foci within the liver. A total of 780,000 new cases and 740,000 deaths have been reported every year,

Corresponding author: Tianyu Zhang, CT Department, The Second Affiliated Hospital of Qiqihar Medical College, No. 37 Zhonghua West Rd, Qiqihar 161000, China.
Tel: +86 0452 2739690, Email: zhangtianyu0819@163.com
Received: 16/02/2021; Accepted: 02/03/2021

with a male-to-female ratio of 4:1 [1]. Early HCC is asymptomatic, so HCC is frequently diagnosed at an advanced stage, which portends a poor prognosis. Microvascular invasion (MVI), a new pathological stage of HCC, is an inducement of early recurrence of HCC, with a high incidence after surgery [2,3]. The recurrence rate of HCC in patients with MVI is significantly higher than those without MVI [4]. As a novel MR technique, dynamic contrast-enhanced magnetic resonance imaging (DCE-MRI) has been confirmed to play an increasingly important role in evaluating liver diseases. DCE-MRI is a functional imaging technique that analyzes the properties of pathological tissues according to the abnormal microvascular system. It measures morphological features of lesions by quantitative and semi-quantitative methods, and microscopically reflects the changes in microcirculation to provide more information about liver lesions. Moreover, it may have the potential to detect micrometastases with unclear morphology. In addition, its ability to distinguish MVI biomarkers facilitates the early diagnosis and prognosis evaluation in HCC.

Vascular endothelial growth factor (VEGF) is a fundamental regulator of angiogenesis [5]. Many members of the VEGF family function differently, and the activation of VEGF receptor is associated with tumor proliferation. Therefore, VEGF-targeted drugs are effective in the treatment of advanced HCC. Furthermore, VEGF can promote angiogenesis by stimulating the proliferation of endothelial cells, and can induce vascular proliferation by reducing immune responses. The VEGF family is composed of VEGF-A, B, C, D, E and placental growth factor. VEGF-B is effective in enhancing vascular endothelial cell growth and migration by binding to its receptor Flt-1, thus accelerating tumor proliferation and metastasis. However, the effects of VEGF in HCC have not been explored.

There is increasing evidence indicating the role of microRNAs (miRs) in regulating biological characteristics of various tumors, such as maintaining cell proliferation, resisting apoptosis, enhancing invasion and inducing angiogenesis. MiRs have been reported to act as effective markers for the diagnosis of HCC. Aberrant expression of miRs plays an important role in many human malignancies [6]. The role of miRs that are abnormally expressed in angiogenesis-related endothelial cells in tumor angiogenesis has been widely studied [7]. There is evidence that miR-155, miR-106b, miR-490-3p, miR-24 and miR-335, which are downregulated in HCC, are promising indicators of diagnosis and prognosis [8]. MiR-497 is located at chromosome 17 P13.1 and is abnormally expressed in neuroblastoma [9], gastric cancer [10], colorectal cancer [11], cervical cancer [12] and breast cancer [13], and the abnormal expression is related to tumor proliferation and apoptosis. Mir-497 may regulate VEGFR2 expression at post-transcriptional level, and its dysregulation may contribute to tumor angiogenesis [14]. Although the abnormal expression of miR-497 has been reported to affect proliferation and migration in HCC, the specific mechanism remains to be elaborated.

Methods

Samples and methods

Fifty-five pairs of cancerous and adjacent tissues were surgically resected in our hospital from 2017 to 2019, then frozen by liquid nitrogen and stored in a refrigerator at -80°C. Imaging data of postoperative specimens collected from HCC patients with MVI (diagnosed by DCE-MRI) were retrospectively analyzed. According to imaging results combined with typical images of tumor capsule and infiltration, low diffusion coefficients and irregular peripheral enhancement, the tumor samples were divided into non-metastatic HCC and HCC with MVI. All pathological samples were confirmed by routine H&E staining and immunohistochemistry (IHC) and the samples were collected with the consent of patients and the Ethics Committee of our hospital.

Inclusion criteria

Patients diagnosed with HCC by DCE-MRI in our hospital from January, 2017 to December, 2019; patients receiving no surgical resection, chemoembolization therapy, , radiotherapy, chemotherapy and immunotherapy before surgery; patients without contraindications to MRI and communication disorders. Patients were diagnosed with HCC and MVI when one of the following signs appeared: 1: Tumor morphology: type I (smooth without nodules), type II (single nodule with extranodal protrusion) and type III (multiple nodules). Type III was considered as the sign of MVI in solitary HCC. 2: Type of capsule: intact capsule, capsule defect, and capsule loss (a sign of MVI). 3: Peritumoral enhancement: The presence of patches or crescent-shaped areas around HCC lesions in the arterial phase and iso- and hypo-intense signals in the portal venous or equilibrium phase was identified as a MVI sign.

Analysis of mRNA expression profiles in HCC by TCGA and CCLE database

Firstly, all the files of gene expression profiles of VEGF-B and their receptor in TCGA database were downloaded using the TCGA-assembler package. Data of 529 gene expression samples (HCC sample, 369; paracancer sample,160) were retrieved. Then, BRB-Arraytools (version v4.5.0Beta2) was used to import the expression profile and gene annotation files to read the gene expression values, which were matched with the follow-up data and analyzed [15]. RNA-seq data from HCC cell lines in CCLE database were downloaded and analyzed statistically by GraphPad8.0.

Cell culture

Human HCC cell lines (HepG2, SMMC-7721) and normal human liver cell line L-02 frozen in our laboratory were removed from liquid nitrogen and melted, centrifuged at 800 rpm for 2 min, resuspended in DMEM containing 10% serum and 1% penicillin-streptomycin, and cultured in a cell incubator (5% CO_2, 37°C).

RNA extraction and real-time PCR

RNA was extracted from tissues and cell lines by TRIzol (Invitrogen, USA) and reverse-transcribed into cDNA with the miR reverse transcription kit (Applied Biosystems, USA). Next, miR-497 levels were quantified using a TaqMan probe and TaqMan universal PCR master Mix (ABI, USA). The reaction was carried out in the ABI StepOne Plus Detection system (ABI Co, USA) under conditions of pre-denaturation at 95°C for 10 min, denaturation at 95°C for 15 s, annealing and extension at 60°C for 1 min, for a total of 40 cycles. Taking RNU6B as the internal reference, each sample was tested in triplicate, and the relative expression of miR-497 was calculated by $2^{-\Delta\Delta CT}$.

Cell transfection

SMMC-7721 cells in logarithmic growth phase were planted in a 6-well plates and cultured for 24 h. miR-497 mimic or miR-497 inhibitor (Shanghai Jima Co) and their negative controls were transfected using the Lipofectamine3000 (Invitrogen, USA) according to the attached instructions. Cells were collected and subjected to subsequent experiments 24 h after transfection. MiR-497 mimic sequence: 5'-CAGCAGCACACUGUGGUUUGU-3', NC sequence: 5'-UUCUCCGAACG UGUCACGUTT-3', miR-497 inhibitor sequence: 5'-ACAAACCACAGUGUGCUGCUG-3', inhibitor NC sequence: 5'-CAGUACUUUUGUGUAGUACAA-3', si-VEGF-B sequence (5'-UGGAUUUGUACCAUUCUUCUG-3', 5'-GAAGAAUGGUACAAAUCCAAG-3').

Western blot (WB)

The transfected cells were taken out of the medium after 48 h, then washed one time with pre-cooled PBS, lysed (25 mmol/L, Tris-Cl pH 7.5), 5 mmol/L EDTA, 1% SDS and 1% protease inhibitor) on ice (shaking once per 10 min for three times), finally centrifuged at high speed to obtain the supernatant. After quantifying by a BCA protein assay kit (Beyotime, China) and electrophoresing in 10% SDS-PAGE, the protein was blotted to a PVDF membrane. Afterwards, the membrane was sealed with 5% skimmed milk powder at room temperature for 1 h and reacted overnight with anti- VEGF-B (GST, 2463, 1: 1000), FLT-1 (Abcam, 9540, 1: 1000) and GAPDH (Abcam, 8245,1:1000) primary antibodies at 4°C. After 3 TBST washes, the membrane was incubated with secondary antibody (CST: anti-rabbit, HRP-linked antibody, #7074, anti-mouse, HRP-linked antibody, 1: 1000) for 1 h. ECL exposure and imaging were performed routinely.

Cell invasion and migration (transwell assay)

A transwell insert (BD Biosciences, USA) of 5 mm pore size was used. DMEM (750 μL) containing 10% FBS and serum-free DMEM suspension (200 μL) containing 5×104 cells were added into the basolateral and apical chambers, respectively. The cells were cultured in an incubator with 5% CO_2 at a constant temperature of 37°C for 48 h. After that, the insert was taken out, and residual matrix glue and cells in the apical chamber were removed with a cotton swab. Migrating and invading cells were fixed in 4% paraformaldehyde and stained with 0.5% crystal violet. After washing away the residual crystal violet solution with PBS, the insert was dried at room temperature. The cells present in 6 random fields were photographed under an inverted microscope (Lecica Leica, x100 times) and counted.

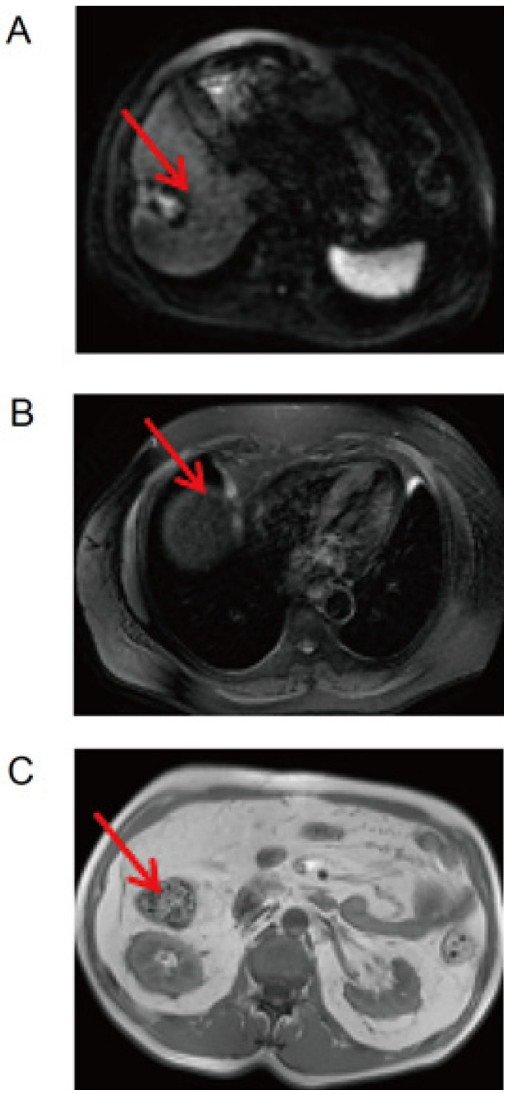

Figure 1. Identification of HCC by dynamic contrast-enhanced MRI. **A:** The DCE-MRI image of the right lobe of the liver shows a type III lesion with multiple nodules. **B:** The DCE-MRI image of the right lobe of the liver shows capsule defect of the lesion. **C:** The DCE-MRI image of the right lobe of the liver shows the presence of patches or crescent-shaped areas around the HCC lesion in the arterial phase and iso- and hypo-intense signals in the portal venous or equilibrium phase. The area marked by the arrows indicates the type of tumor.

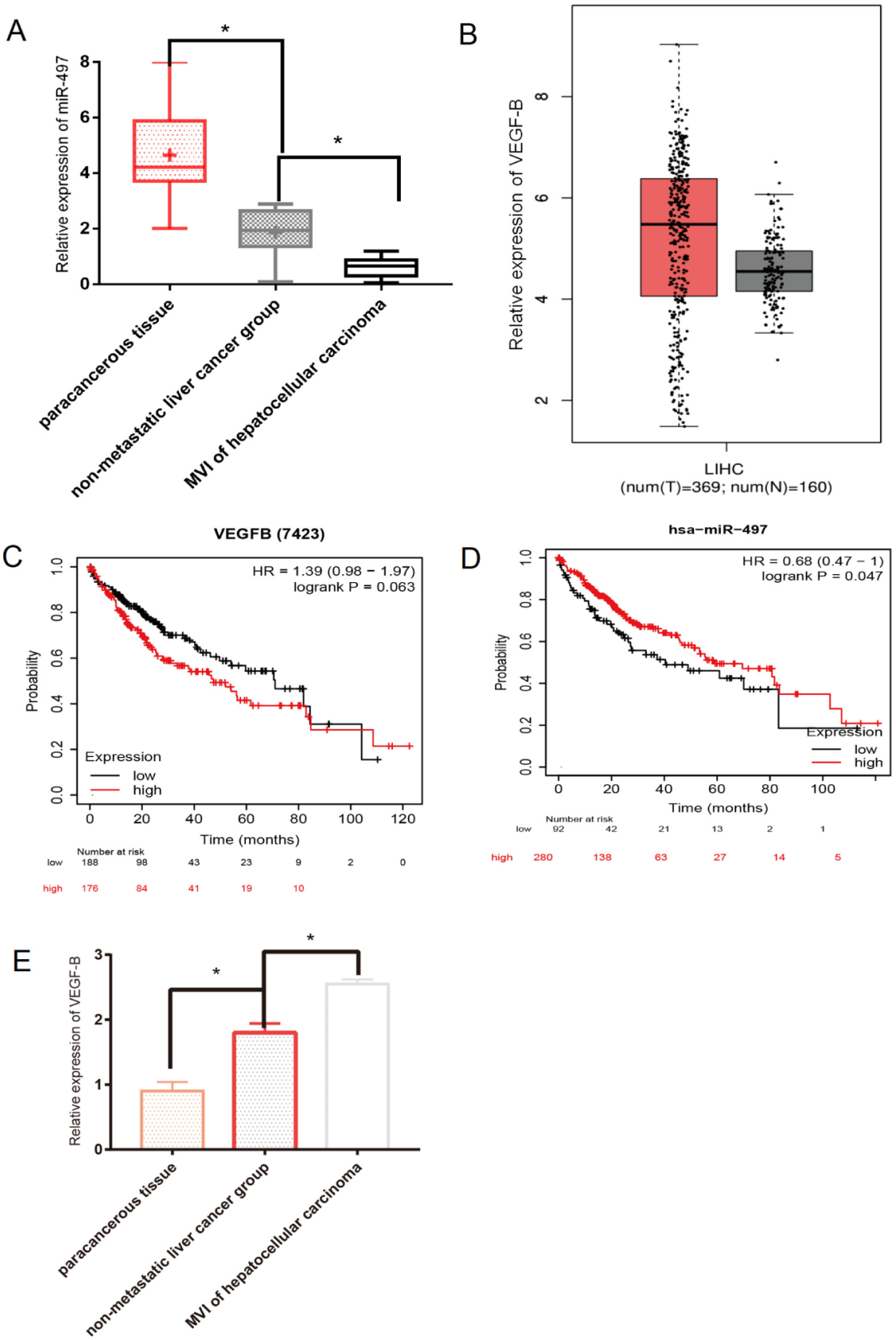

Figure 2. Expression of miR-497 and VEGF-B in HCC tissues and its relation to prognosis. **A:** miR-497 expression is quantified in patients with HCC with MVI and without MVI, and in adjacent tissues by Q-PCR. **B:** TCGA database demonstrates that VEGF-B expression in HCC tissues is higher than that in adjacent tissues. **C** and **D:** Survival curves (http://gepia.cancer-pku.cn/index.html) are plotted by analyzing the data in TCGA database. **E:** VEGF-B expression is quantified in patients with HCC with MVI and without MVI, and in adjacent tissues by Q-PCR. Each test was independently repeated in triplicate, and the data were tested by t-test. (*p<0.05).

Cell proliferation (MTT assay)

Modified MTT assay was used to quantify cell proliferation. SMMC-7721 cells (50-60% density) transfected with 100 nM miR-497 mimic, miR-497 inhibitor or inhibitor-NC were incubated in 96-well plates at 37°C for 48 h, with untransfected cells as control. MTT solution (20 μL) was added to each well prior to a 4-h incubation. The supernatant was removed and cells were treated with 150 μL/well dimethyl sulfoxide. Optical density (OD) values at 570 nm were measured with a 96-well microplate reader. The MTT assay was repeated three times. The inhibition rate ([OD value in control group - OD value in treatment group]/OD value in control group x 100%) was calculated and cell growth curves were plotted.

Dual-luciferase reporter (DLR) assay

SMMC-7721 cells were inoculated in 24-well plates with 2×10^5 cells per well. On the second day, 80 ng pMIR-REPORTER luciferase vectors containing 3'UTR of FLT-1 (with miR-497 binding site wild-type or mutant), PRL-TK control (encoding Renilla luciferase, 8 ng) and miR-497mimic or mimic NC (final concentration of 50 nm) were co-transfected using the liposome 2000 (Invitrogen). Renilla (RLuc) and Firefly luciferases (FLuc) were measured by a DLR kit (Promega, USA) one day post-transfection. The results were expressed as the ratio of RLuc to FLuc. Each test in each group was repeated at least three times.

Statistics

The tests in each group were repeated independently in triplicate, and all data was statistically analyzed with GraphPad 8.0. Continuous data was expressed by mean±standard deviation, and inter- and intra-group comparisons were conducted with t-test. Categorical data was analyzed by chi-square test. Pearson's linear correlation was employed to identify the correlation between gene expression levels. Statistical significance was set at $p\leq0.05$.

Results

Identification of HCC and determination of HCC with MVI

At present, considerable attention has been devoted to the integration of quantitative, multiparameter and functional imaging data in the field of oncology. Here, imaging data of postoperative specimens collected from HCC patients with MVI (diagnosed by DCE-MRI) was retrospectively analyzed. Images were shown in Figure 1A: HCC focus demonstrates a sign of MVI in solitary HCC-type III morphology with multiple nodules; Figure 1B: The DCE-MRI image of the right lobe of the liver shows a sign of MVI in HCC-capsule defect; Figure 1C: The DCE-MRI image shows a sign of MVI-iso- and hypo-intense signals in the portal venous or equilibrium phase.

High expression of VEGF-B portends a poor prognosis in HCC

Through statistical analysis of data of HCC collected in TCGA database, we found that miR-497 expression in cancer tissues was lower than that in adjacent tissues, which portended a poor prognosis (Figures 2A, C). Also, VEGF-B was highly expressed in HCC and the overall survival of patients remained low (Figures 2B,C). Therefore, we hypothesized that miR-497 expression was lower in patients with HCC with MVI than those without

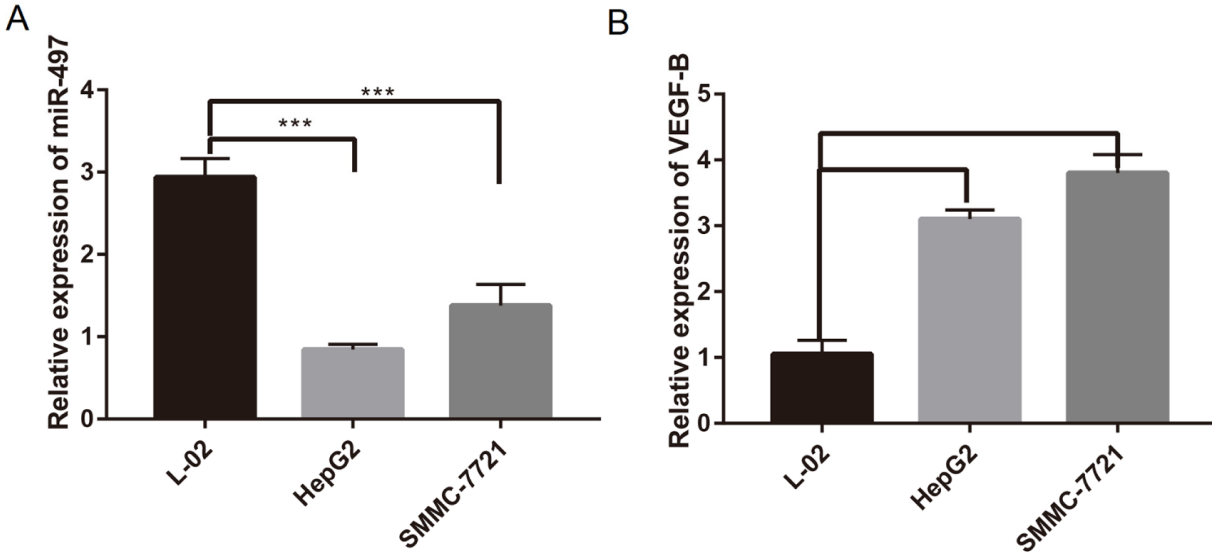

Figure 3. Expression of miR-497 in HCC cell lines. **A** and **B:** Q-PCR shows that miR-497 expression in HCC cell lines is lower, and VEGF-B expression is higher than that in the normal liver cell line (*p<0.001).

MVI, accompanied by elevated levels of VEGF-B. To verify this, we quantified the relative expression of miR-497 and VEGF-B in patients with MVI and without MVI by quantitative PCR (Q-PCR), and the results were consistent with our hypothesis (Figures 2E.F). Therefore, we further speculated that miR-497 may be able to regulate the expression of VEGF-B.

Expression of miR-497 in HCC cell lines

After analyzing CCLE database data, the expression of miR-497 and VEGF-B in HepG2 and SMMC-7721 cell lines was determined by Q-PCR. It turned out that miR-497 presented a lower expression in HCC cell lines compared with the normal liver L-02 cell line (Figure 3A); in addition, miR-497 expression was associated with the invasiveness of HCC. VEGF-B expression was negatively correlated with miR-497 expression (Figure 3B) and FLT-1 was highly expressed in HCC cell lines.

miR-497 inhibits proliferation and migration of HCC cells

Cancers cannot be cured completely for their strong migratory and invasive properties. Therefore, we transfected miR-497 mimic and inhibitor into SMMC-7721 and HepG2 cells. Changes in

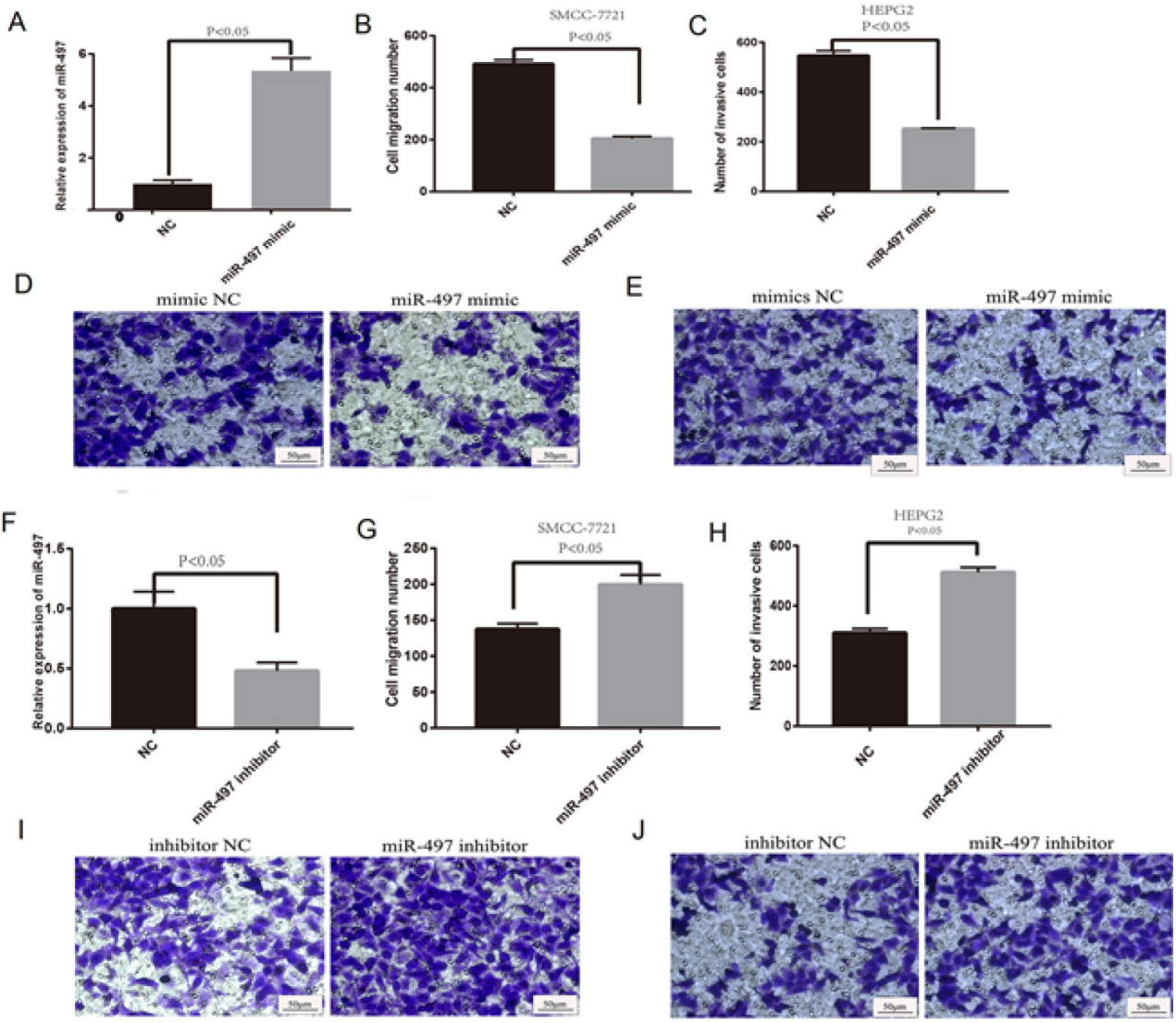

Figure 4. The effect of miR-497 on invasion and migration of HCC cells. **A:** miR-497 expression after miR-497 mimic transfection is verified by Q-PCR. **B** and **C:** Quantitative results on migration experiments. **D:** Migration of SMMC-7721 cells decreased after transfection with miR-497 mimic. **E:** Invasion of SMMC-7721 cells decreased after transfection with miR-497 mimic. **F:** miR-497 expression after miR-497 inhibitor transfection is verified by Q-PCR. **G** and **H:** Quantitative results of invasion experiments. **I:** Migration of SMMC-7721 cell after transfection with miR-497 inhibitor. **J:** Invasion of SMMC-7721 cells enhanced after transfection with miR-497 inhibitor. Each test was independently repeated in triplicate, and the data are were by t-test (*p<0.05).

proliferation, invasion and metastasis of SMMC-7721 cells were determined by MTT, transwell assay and wound healing assay. The proliferation of cells transfected with miR-497 mimic significantly decreased, but transfection with miR-497 inhibitor had no inhibitory effect on the proliferation. Transwell assay indicated that after overexpression of miR-497, the number of invading SMMC-7721 cells decreased dramatically, but miR-497 downregulation increased the number of invading cells. Through the wound healing assay, we found that the migration of SMMC-7721 cells was weakened after overexpression of miR-497, while the opposite result was obtained after miR-497 downregulation. Therefore, we concluded that miR-497 inhibited proliferation and invasion of HCC cells. Details are shown in Figure 4.

DLR assay confirms the relationship between miR-497 and VEGF-B

To verify that miR-497 may inhibit FLT-1 expression by directly interacting with the predicted binding site of VEGF-B 3'-UTR, the cDNA 3'-UTR fragment was cloned into the luciferase reporter vector from VEGF-B mRNA containing miR-497 binding sequences. In addition, another luciferase reporter gene fused with VEGF-B 3'UTR was established, but containing a mutant binding sequence of miR-497. Then, we transfected the luciferase reporter vectors with wild-type or mutant miR-497 binding sequences into SMMC-7721 cells. The cells were co-transfected miR-497 mimic or mimic control to determine the luciferase activity. As shown in Figure 5, miR-497 mimic at a concentration of 50 nM inhibited the luciferase activity of

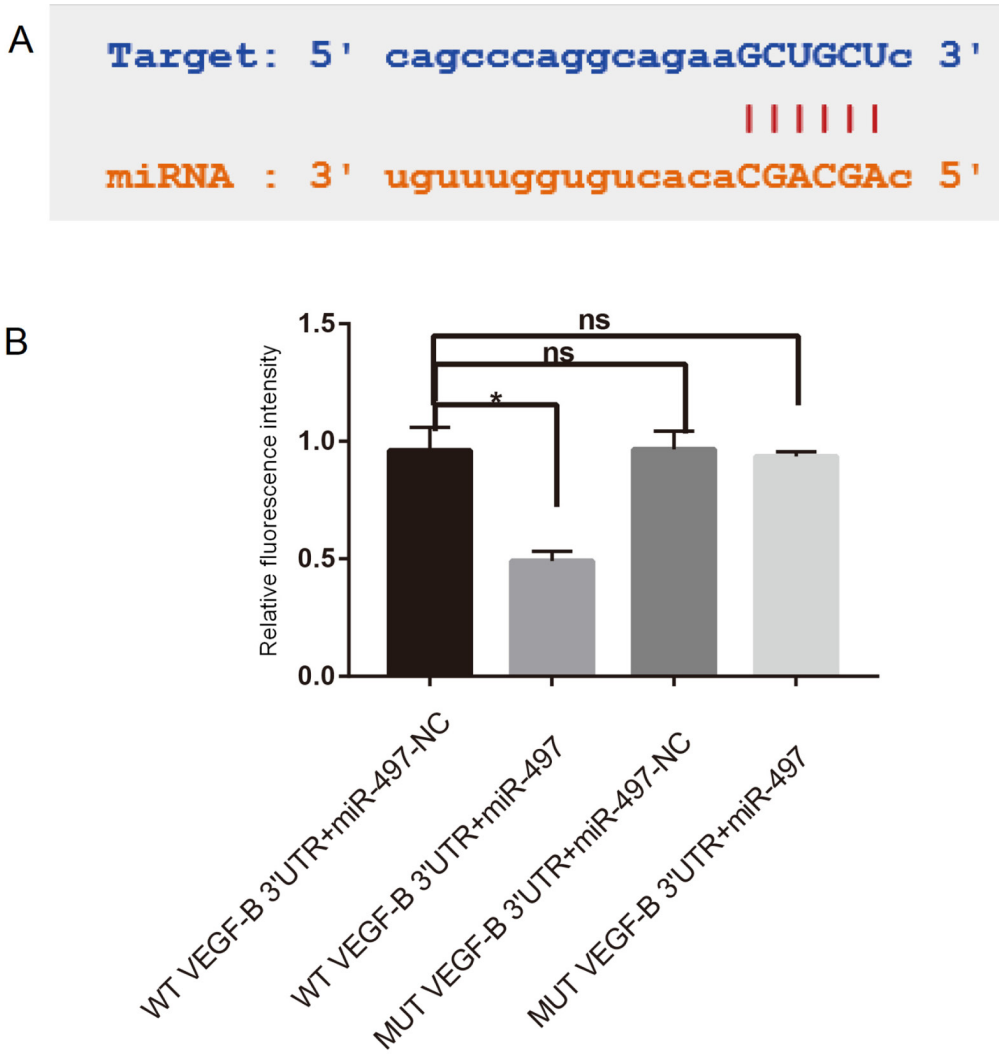

Figure 5. Luciferase activity in cells co-transfected with WT VEGF-B-1 3'-UTR or mut VEGF-B 3' -UTR and miR-497mimic or miR-497 NC. **A:** Targeting sequences of miR-497 and VEGF-B. **B:** VEGF-B was the target gene of miR-497 (DLR assay). Each test was independently repeated in triplicate, and the data are tested by t test (*p<0.05, ns: non significant)

the reporter vector containing binding sequences of miR-497. However, it showed no significant effect on the vector containing mutant sequence. These data suggested that miR-497 may inhibit the translation of VEGF-B by directly acting on miR-497-specific response elements in the 3'-UTR of VEGF-B of SMMC-7721 cells. This further confirmed that miR-497 regulated the metastasis of HCC cells by targeting and inducing the low expression of VEGF-B.

miR-497 regulates VEGF-B pathway in HCC

The VEGF family consists of VEGF-A, B, C, D, E and embryonic growth factor that participates in angiogenesis [16]. Angiogenesis contributes to tumor growth. Although VEGF-A is the most widely studied member of this family, the abnormal expression of VEGF-B in malignant tumors has also been reported [17]. VEGF-B expression is associated with tumor staging and formation of capsule or bile duct in HCC, but whether VEGF-B pathway is involved in invasion and migration remains unknown. Compared with the NC group, the expression of VEGF-B in miR-497 mimic group was downregulated in SMMC-7721 cells. To further verify the experimental result, we used miR-497 inhibitor to interfere with the expression of miR-497. Western blot showed that VEGF-B expression in miR-497 inhibitor group was higher than that in blank group. Therefore, miR-497 affected the invasion and migration of HCC cells by regulating VEGF-B pathway (Figure 6).

miR-497 affects VEGF-B receptor-FLT-1 pathway in HCC

In the pathological and physiological studies of tumors and embryos, it is found that VEGF mainly transmits the information of promoting vascular proliferation via FLT-1 [18]. VEGF-B and its receptor FLT-1 regulate the angiogenesis in malignant tumors [19] and the lymph node metastasis in breast cancer [20]. The combination of the two affects the growth and metastasis of tumors and promotes vascular endothelial growth. Therefore, we constructed a HCC cell line with miR-497 overexpression to evaluate the regulatory effect of miR-49 on FLT-1. Lower expression of FLT-1 was observed in miR-497 overexpression group, while

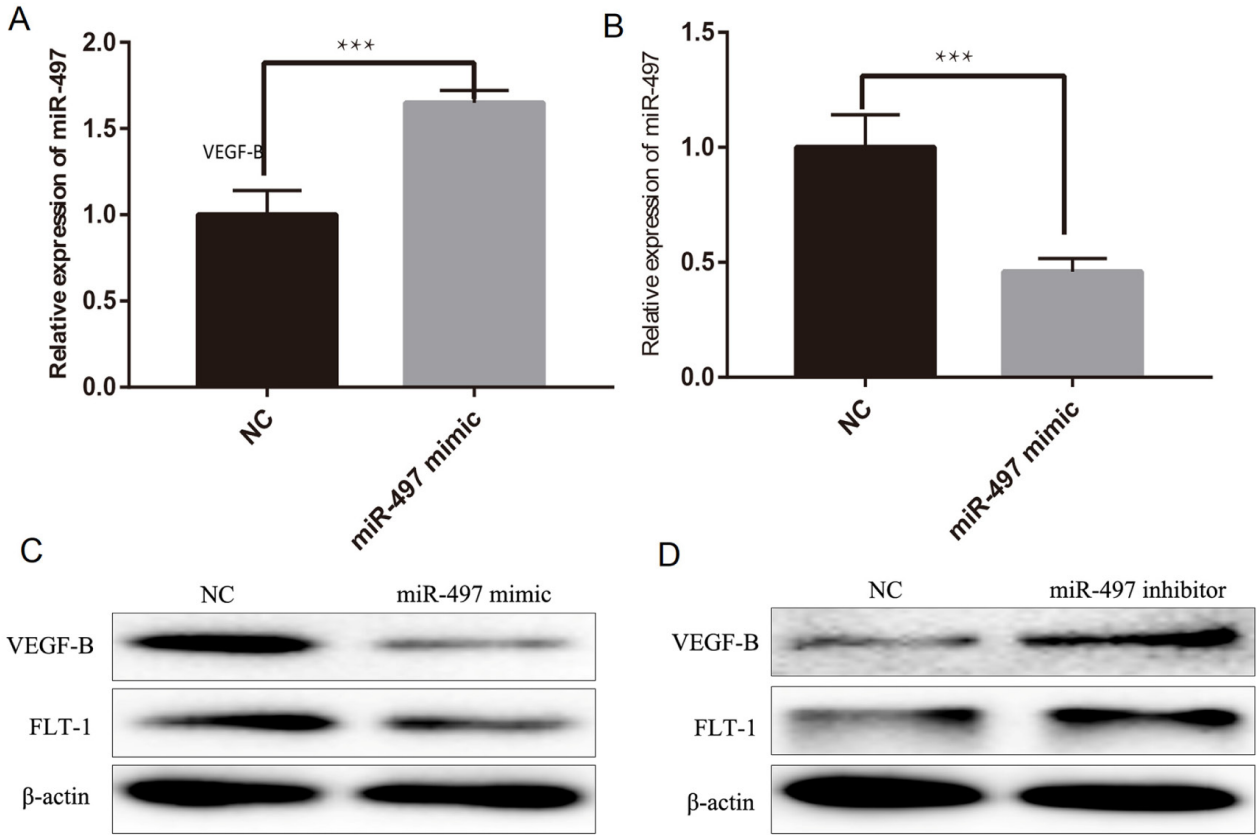

Figure 6. miR-497 regulates the expression of VEGF-B in HCC cell lines. **A:** Overexpression of miR-497 (Q-PCR). **B**: Knockdown of miR-497 (Q-PCR). **C:** Overexpression of miR-497 inhibits VEGF-B levels (WB). **D:** Downregulation of miR-497 increased VEGF-B levels. Each test was independently repeated in triplicate, and the data were tested by t-test (*p<0.05).

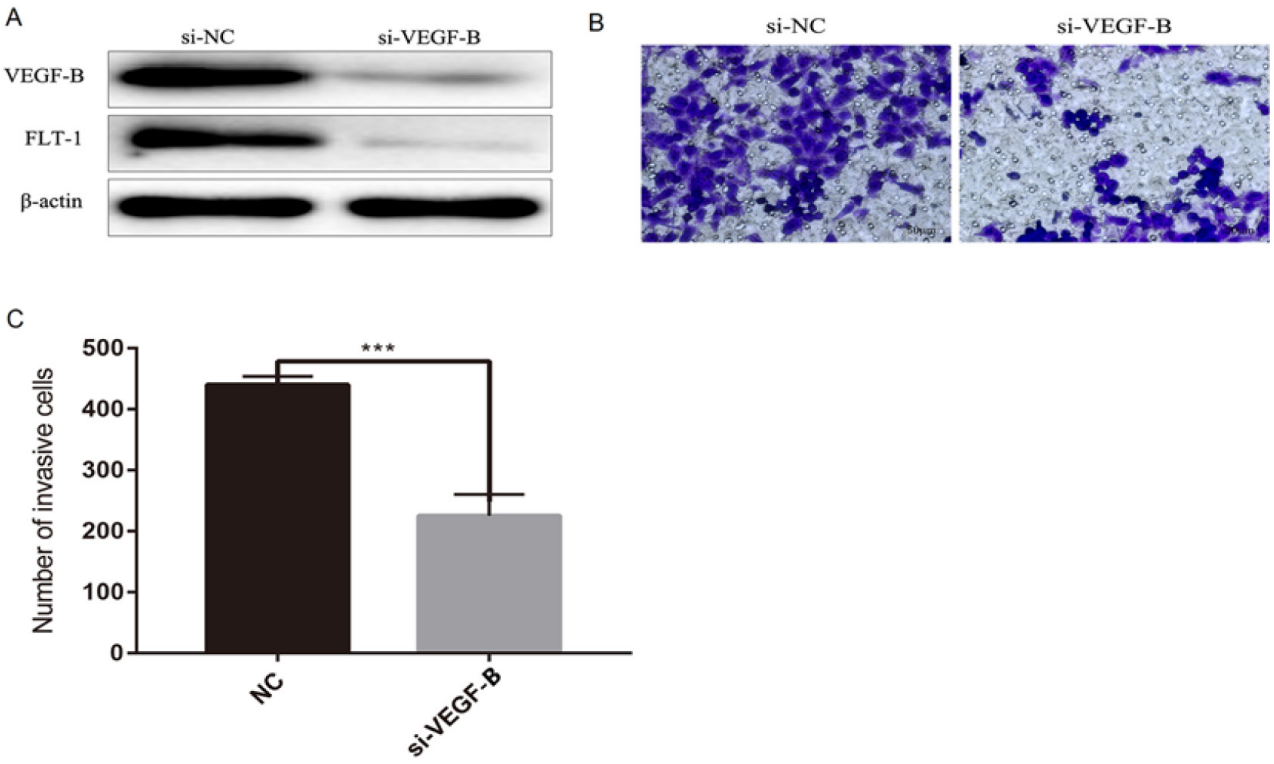

Figure 7. miR-497 regulates the expression of FLT-1 in HCC cell lines. **A:** Transient transfection of si-VEGF-B downregulated FLT-1. **B:** Effects of si-VRGF-B and si-NC on invasion and migration of SMMC-7721 cells. Each test was independently repeated in triplicate, and the data were tested by t-test C***p<0.005). **C:** Quantitative results of Figure 7B.

an opposite result was obtained in the miR-497 inhibitor group. Thus, miR-497 regulated VEGF-B through VEGF-B pathway to influence the invasion in HCC. Afterwards, we explored the effects of si-VEGF-B-1 and si-NC on invasion and migration of SMMC-7721 cells. After transfection of si-VEGF-B-1, a significant weakening in invasion and migration was noticed. It was concluded that miR-497 targeted VEGF-B to influence the invasion and migration of HCC cells (Figure 7).

Discussion

Strong migratory and invasive properties are the fundamental causes of the incurability of cancers. Accumulating evidence has indicated the involvement of miRs in the regulation of tumor invasion and metastasis, expecting to serve as targets for the diagnosis and treatment [21]. The molecular mechanism of miR-497 in the progression of HCC has not been fully elucidated. Herein, imaging data of postoperative specimens collected from HCC patients with MVI (diagnosed by DCE-MRI) was analyzed. DCE-MRI is a functional imaging technique to evaluate the physiological properties of pathological tissues according to the disordered microvascular system. It not only provides the morphological information of lesions, but also reflects the changes in microcirculation, leading to a better understanding of liver lesions. The downregulation of miR-146a may restrict the invasion and metastasis of HCC cells by downregulating VEGF expression via VEGF-B pathway. In addition, miRs, including miR-195, miR-101 and miR-20b, can regulate VEGF pathway through gene silencing. In the present study, postoperative specimens were collected from HCC patients with MVI diagnosed by DCE-MRI [22]. MiR-497 expression in HCC tissues was lower than that in adjacent tissues, and decreased more significantly in HCC patients with MVI than those without MVI. Since there is no standard to distinguish invasion and migration of HCC cell lines, we selected SMMC-7721 and HEPG2 cells for analysis. Compared with the normal liver cell line (L-02), the expression of miR-497 decreased in HCC cell lines. According to the data retrieved from TCGA database, miR-497 expression was related to the survival of patients with HCC. Overexpression of miR-497 inhibited proliferation, migration and invasion of SMMC-7721 cells. VEGF-B, upregulated in HCC, has been identified as a new target of miR-497 in HCC patients with MVI, which was confirmed in the present study by the DLR assay. MiR-497 acts as a

tumor suppressor in several common malignant tumors. In addition, long intergenic non-protein coding RNA152 accelerates multiple myeloma through negative regulation of miR-497 [23]. Moreover, miR-497 induces cell cycle arrest of HCC cells at G0/G1 phase by targeting and regulating the expression of CyclinD3 and CDK6, thereby slowing HCC progression [24]. In cervical cancer, miR-497 targets the insulin-like growth factor-1 receptor (IGF-1R) to play a role in tumor inhibition, and it also targets cyclin E1 to inhibit the proliferation of HeLa cells [25], indicating its potential as a prognostic marker. In non-small cell lung cancer, miR-497 inhibits YAP1 and thus suppresses tumor growth [26]. The involvement of miR-497 in epigenetic regulation of tumors has also been reported. Flt-1, a cell surface receptor of VEGF, plays a pivotal role in the cardiovascular system, hematopoietic system, tumor proliferation and embryo development. In human umbilical vein endothelial cells (HUVECs) and HEK293 cells, expression of Flt1 is suppressed by metalloproteinase inhibitors [27]. The N-terminal cleavage and release of Flt1 extracellular domain is mediated by ADAM10 and ADAM17, and regulated by VEGFR2 and Flt1 intracellular domain. There is evidence that Flt-1 participates in the regulation of tumor neovascularization as a target gene of VEGF. For example, VEGF-A inhibits the cleavage of FLT1 extracellular domain through VEGF receptor 2 (KDR) in a time- and dose-dependent manner [28].

HCC is different from other malignant tumors for its hypervascularity. MVI is common in HCC and has a high incidence. Pre-treatment prediction of MVI is helpful to guide surgical treatment strategies, and postsurgical pathologic confirmation is helpful to examine recurrence and distant metastasis. However, the pathogenesis of MVI has not been fully understood, so postoperative pathological diagnosis remains the first choice. DCE-MRI is a relatively new technique for the diagnosis and treatment of HCC. At present, the treatment of HCC still relies on surgical resection, but this is effective only for early-staged tumors. The efficacy of traditional radiotherapy and chemotherapy is unsatisfactory, coupled with drug resistance of the tumor and frequent recurrence and distant metastasis after surgery. Therefore, inhibiting tumor metastasis and recurrence and understanding the mechanism of drug resistance are critical for the development of novel treatment options. Sorafenib, the first systemic molecular targeted drug approved by FDA for first-line treatment of unresectable HCC, is a multi-tyrosine kinase inhibitor [29]. Subsequently, in July 2018, an oral tyrosine kinase inhibitor lenvatinib was approved by FDA [30] for the treatment of patients with HCC who initially receive chemotherapy. Immunotherapies have been considered as an effective treatment for patients with advanced HCC. Several new immunotherapies, including the use of checkpoint inhibitors, new immune cells and miRs, have been applied in clinical trials to treat HCC. However, there are still concerns largely unsolved. Other therapeutic schemes, including gene therapy, cytotoxic chemotherapy, radiotherapy, hormone therapy and traditional Chinese medicine therapy, also produce unsatisfactory results. Therefore, it is necessary to reveal new molecular mechanisms of the occurrence and development of HCC and to develop novel targeted therapies.

MVI in HCC is a response to phenotypic and characteristic changes from a microscopic point of view, with high incidence. The pathological features of MVI have been confirmed, that is, small branches of hepatic vein or portal vein adjacent to the tumor. MVI is a process in which cancer cells gradually destroy the surrounding tissues through cloning and proliferation, invasion of surrounding matrix, thrombus exfoliation, and tumor enlargement and metastasis. Prediction of MVI is the current research focus, and looking for related indicators can facilitate the diagnosis and treatment of HCC. Our study revealed the high expression of miR-497 in HCC patients with MVI, and the lower the degree of tumor differentiation, the higher the MVI incidence. Exploration of the correlation between miR-497 expression and MVI may be valuable for predicting the survival of patients with HCC.

Overall, the finding that miR-497 inhibits invasion and migration of HCC cells by targeting VRGF-B inspires the diagnosis and treatment of HCC, contributing to the development of related pathway inhibitors.

Acknowledgement

This study was supported by Qiqihar Medical College Academy of Sciences Fund Project (QMSI2019M-27).

Conflict of interests

The authors declare no conflict of interests.

References

1. Forner A, Reig M, Bruix J. Hepatocellular carcinoma. Lancet 2018; 391:1301-14.
2. Zhang Z, Teng M, Xu Z, et al. Correlations of HACE1 expression with pathological stages, CT features and prognosis of hepatocellular carcinoma patients. J BUON 2020;25:2570-5.
3. Lim KC, Chow PK, Allen JC et al. Microvascular invasion is a better predictor of tumor recurrence and overall survival following surgical resection for hepatocellular carcinoma compared to the Milan criteria. Ann Surg 2011; 254:108-13.
4. Hu HT, Shen SL, Wang Z et al. Peritumoral tissue on preoperative imaging reveals microvascular invasion in hepatocellular carcinoma: a systematic review and meta-analysis. Abdom Radiol (NY) 2018; 43:3324-30.
5. Facciuto ME, Singh MK, Rochon C et al. Stereotactic body radiation therapy in hepatocellular carcinoma and cirrhosis: evaluation of radiological and pathological response. J Surg Oncol 2012; 105:692-698.
6. Facciuto ME, Singh MK, Rochon C et al. Stereotactic body radiation therapy in hepatocellular carcinoma and cirrhosis: evaluation of radiological and pathological response. J Surg Oncol 2012; 105:692-8.
7. Yoo JK, Jung HY, Lee JM et al. The novel miR-9500 regulates the proliferation and migration of human lung cancer cells by targeting Akt1. Cell Death Differ 2014; 21:1150-9.
8. Zhou B, Ma R, Si W et al. MicroRNA-503 targets FGF2 and VEGFA and inhibits tumor angiogenesis and growth. Cancer Lett 2013; 333:159-69.
9. Yadav S, Pandey A, Shukla A et al. miR-497 and miR-302b regulate ethanol-induced neuronal cell death through BCL2 protein and cyclin D2. J Biol Chem 2011; 286:37347-57.
10. Zhu W, Zhu D, Lu S et al. miR-497 modulates multidrug resistance of human cancer cell lines by targeting BCL2. Med Oncol 2012; 29:384-91.
11. Guo ST, Jiang CC, Wang GP et al. MicroRNA-497 targets insulin-like growth factor 1 receptor and has a tumour suppressive role in human colorectal cancer. Oncogene 2013; 32:1910-20.
12. Zheng D, Radziszewska A, Woo P. MicroRNA 497 modulates interleukin 1 signalling via the MAPK/ERK pathway. FEBS Lett 2012; 586:4165-72.
13. Shen L, Li J, Xu L et al. miR-497 induces apoptosis of breast cancer cells by targeting Bcl-w. Exp Ther Med 2012; 3:475-80.
14. Tu Y, Liu L, Zhao D et al. Overexpression of miRNA-497 inhibits tumor angiogenesis by targeting VEGFR2. Sci Rep 2015; 5:13827.
15. Chen J, Liu A, Wang Z et al. LINC00173.v1 promotes angiogenesis and progression of lung squamous cell carcinoma by sponging miR-511-5p to regulate VEGFA expression. Mol Cancer 2020; 19:98.
16. El Shorbagy S, abuTaleb F, Labib HA et al. Prognostic Significance of VEGF and HIF-1 alpha in Hepatocellular Carcinoma Patients Receiving Sorafenib Versus Metformin Sorafenib Combination. J Gastrointest Cancer 2020;52:269-79.
17. Bellomo D, Headrick JP, Silins GU et al. Mice lacking the vascular endothelial growth factor-B gene (Vegfb) have smaller hearts, dysfunctional coronary vasculature, and impaired recovery from cardiac ischemia. Circ Res 2000; 86:E29-35.
18. Zhao Q, Wu CS, Fang Y et al. Glucocorticoid Regulates NLRP3 in Acute-On-Chronic Hepatitis B Liver Failure. Int J Med Sci 2019; 16:461-9.
19. Mousavi SA, Skjeldal F, Fønhus MS et al. Receptor-Mediated Endocytosis of VEGF-A in Rat Liver Sinusoidal Endothelial Cells. Biomed Res Int 2019; 2019:5496197.
20. Samadi P, Saki S, Dermani FK, Pourjafar M, Saidijam M. Emerging ways to treat breast cancer: will promises be met? Cell Oncol (Dordr) 2018; 41:605-21.
21. Peng X, Luo R, Li J et al. Zingiberene targets the miR-16/cyclin-B1 axis to regulate the growth, migration and invasion of human liver cancer cells. J BUON 2020;25:1904-10.
22. Boss MK, Muradyan N, Thrall DE. DCE-MRI: a review and applications in veterinary oncology. Vet Comp Oncol 2013; 11:87-100.
23. Feng F, Kuai D, Wang H et al. Reduced expression of microRNA-497 is associated with greater angiogenesis and poor prognosis in human gliomas. Hum Pathol 2016; 58:47-53.
24. Tu Y, Liu L, Zhao D et al. Overexpression of miRNA-497 inhibits tumor angiogenesis by targeting VEGFR2. Sci Rep 2015; 5:13827.
25. Luo M, Shen D, Zhou X, Chen X, Wang W. MicroRNA-497 is a potential prognostic marker in human cervical cancer and functions as a tumor suppressor by targeting the insulin-like growth factor 1 receptor. Surgery 2013; 153:836-47.
26. Han J, Huo M, Mu M, Liu J, Zhang J. [miR-497 suppresses proliferation of human cervical carcinoma HeLa cells by targeting cyclin E1]. Xi Bao Yu Fen Zi Mian Yi Xue Za Zhi 2014; 30:597-600.
27. Huang C, Ma R, Yue J, Li N, Li Z, Qi D. MiR-497 Suppresses YAP1 and Inhibits Tumor Growth in Non-Small Cell Lung Cancer. Cell Physiol Biochem 2015; 37:342-52.
28. Waltenberger J, Claesson-Welsh L, Siegbahn A, Shibuya M, Heldin CH. Different signal transduction properties of KDR and Flt1, two receptors for vascular endothelial growth factor. J Biol Chem 1994; 269:26988-95.
29. Liu Z, Lin Y, Zhang J et al. Molecular targeted and immune checkpoint therapy for advanced hepatocellular carcinoma. J Exp Clin Cancer Res 2019; 38:447.
30. Sun W, Cabrera R. Systemic Treatment of Patients with Advanced, Unresectable Hepatocellular Carcinoma: Emergence of Therapies. J Gastrointest Cancer 2018; 49:107-15.